

Optimal Inspection Scheduling of Steel Bridges Using Nondestructive Testing Techniques

Hsin-Yang Chung¹; Lance Manuel²; and Karl H. Frank³

Abstract: A probabilistic approach is proposed to help select the most suitable nondestructive inspection (NDI) technique and associated optimal schedule for fracture-critical member/detail fatigue inspections on a specific steel bridge. The probability of detection (POD) function for the NDI technique, which is a measure of the detection accuracy, is employed. By combining probability calculations based on use of the POD function together with numerical Monte Carlo simulations of the crack propagation of the fracture-critical detail, a cost function is formulated that includes the expected cost of inspections and failure resulting from the chosen NDI technique and alternative inspection schedules. In summary, the selection of an NDI technique with an associated inspection schedule for fracture-critical inspections is formulated as an optimization problem that can guarantee minimum total cost. The inspection frequency is determined as part of the optimization that utilizes appropriate constraints on inspection intervals and a minimum acceptable (target) structural safety level. A case study for a box girder bridge is presented to demonstrate the application of the proposed probabilistic method.

DOI: 10.1061/(ASCE)1084-0702(2006)11:3(305)

CE Database subject headings: Probability; Nondestructive tests; Monte Carlo method; Bridges, steel; Fractures; Inspection.

Introduction

Steel bridges, an important part of the nation's transportation infrastructure, are vulnerable to fatigue deterioration because of repetitive traffic-loading cycles that they experience. Nondestructive inspection (NDI) techniques, which can detect changes in material properties and/or flaws in structural details without impairing their use, are commonly used to detect and measure cracks in fracture-critical members of steel bridges. The various NDI techniques suggested for use on steel bridges in the Federal Highway Administration's (FHWA) "Bridge Inspector's Training Manual" (Hartle et al. 1995) include ultrasonic inspection (UI), magnetic particle inspection (MI), penetrant inspection (PI), radiographic inspection (RI), acoustic emission inspection (AEI), and visual inspection (VI). Inspection accuracy, accessibility, frequency, cost, and consequences of detection failures (misses) or false indications (false calls) must all be considered when selecting an NDI technique. Though other reliability-based fatigue inspection scheduling methods include consideration for inspection quality, such as those proposed for the offshore industry by Sorensen et al. (1991), Faber et al. (1992), and Cramer and Friis-Hansen (1992), it is not practical to calibrate

inspection quality coefficients and other parameters in their models so as to prescribe use of any single NDI technique (over alternatives). Also, these methods generally demand complicated reliability algorithms or large numerical-simulation studies to obtain optimal inspection results; this limits their applicability to bridge maintenance with associated tighter budgetary constraints.

An intuitive probabilistic approach for dealing with inspection quality is proposed here for selection of the most economical NDI method. On completion of each analysis that involves Monte Carlo simulations, the method recommends a single NDI technique and accompanying inspection schedule for fracture-critical members in a steel bridge that guarantees a specified acceptable safety level through the planned service life of the bridge. The actual probability of detection (POD) functions associated with the various NDI techniques are employed as the NDI detachabilities. By combining probability calculations based on the use of the POD functions together with Monte Carlo simulations of the crack growth for the fracture-critical member, a cost function is formulated that includes the expected cost of inspections and failure that result with each alternative NDI technique and inspection schedule. The selection of an NDI technique with an associated inspection schedule for use in the fracture-critical inspections is modeled as an optimization problem; the POD function and the inspection interval are optimization variables. With appropriate constraints on inspection intervals and on a minimum (target) safety level, an optimal combination of NDI technique and inspection schedule that yields the minimum total cost and ensures the prescribed acceptable safety level for the specified detail can be obtained.

¹Assistant Professor, Dept. of Civil Engineering, National Cheng Kung Univ., No. 1 Ta-Hsueh Road, Tainan City 701, Taiwan. E-mail: hychung@mail.ncku.edu.tw

²Associate Professor, Dept. of Civil Engineering, Univ. of Texas at Austin, Austin, TX 78712 (corresponding author). E-mail: lmanuel@mail.utexas.edu

³Professor, Dept. of Civil Engineering, Univ. of Texas, Austin, TX 78712. E-mail: kfrank@uts.cc.utexas.edu

Note. Discussion open until October 1, 2006. Separate discussions must be submitted for individual papers. To extend the closing date by one month, a written request must be filed with the ASCE Managing Editor. The manuscript for this paper was submitted for review and possible publication on August 10, 2004; approved on December 17, 2004. This paper is part of the *Journal of Bridge Engineering*, Vol. 11, No. 3, May 1, 2006. ©ASCE, ISSN 1084-0702/2006/3-305-319/\$25.00.

Probability of Detection

The four possible outcomes—true positive (hit), false negative (miss), false positive (false call), and true negative (correct accept)—of any NDI procedure are illustrated in Table 1. The POD of a crack of a given size is the conditional probability of a

Table 1. Four Possible Outcomes of Any NDI Procedure

Does crack exist?		Is crack detected by NDI?	
Yes	No	Yes	No
True positive (hit or correct reject)	False positive (false call)	True positive (hit or correct reject)	False negative (miss)
False negative (miss)	True negative (correct accept)	False positive (false call)	True negative (correct accept)

true positive call given that a crack with that size exists. Hence, from repeated inspections, an estimate of the POD can be obtained as follows:

$$\hat{POD} = \frac{N_{TP}}{N_{TP} + N_{FN}} \quad (1)$$

where \hat{POD} =POD estimate for a specific crack size; N_{TP} =number of true positive calls; and N_{FN} =number of false negative calls. Correspondingly, the false call probability (FCP) can also be evaluated as

$$\hat{FCP} = \frac{N_{FP}}{N_{FP} + N_{TN}} \quad (2)$$

where \hat{FCP} =FCP estimate for a specific crack size; N_{FP} =number of false positive calls; and N_{TN} =number of true negative calls.

After introducing cracks of various sizes into test specimens and performing inspections, POD estimates for various crack sizes and different NDI techniques can be obtained. Based on the inspection results, generally, two analysis approaches—the hit/miss method and the signal response method—are employed to formulate the POD function, $POD(a)$, for any crack size, a , with any NDI technique.

Hit/Miss Method

This method is applied when inspection data are recorded in terms of hits or misses (i.e., indications of whether or not a crack is detected). This is commonly used, for example, for data from penetrant inspection and visual inspection tests. The basic idea behind this method is to estimate the probability of detection, \hat{POD} , for any given crack size from the hit and miss data by applying regression analysis or a maximum likelihood procedure. Berens and Hovey (1981) proposed that the log-logistic function can provide a satisfactory model for hit/miss inspection data. The log-logistic POD function can be expressed as

$$POD(a) = \frac{\exp[\alpha + \beta \cdot \ln a]}{1 + \exp[\alpha + \beta \cdot \ln a]} \quad (3)$$

where a =crack size; and α and β =statistical parameters to be estimated.

Because of the binomial property of hit/miss data, the \hat{POD} estimate for a fixed crack size is essentially the sample proportion of hits. So, for a large number of inspections, M , performed for a particular crack size, the distribution of \hat{POD} can be approximated by a normal distribution with mean and variance as follows:

$$E[\hat{POD}] = POD \quad (4)$$

$$Var[\hat{POD}] = \sqrt{\frac{POD(1 - POD)}{M}} \quad (5)$$

In order to have a representative POD function for any NDI technique, reliable \hat{POD} estimation for each crack size is necessary. It is useful then to establish the required number of inspections, M_{req} , that will provide, say, $100(1 - \alpha) \%$ confidence that the error in using \hat{POD} to estimate POD will be less than a specified level E . This required number of inspections, M_{req} , can be determined as follows (Johnson 2000)

$$M_{req} = \frac{1}{4} \left[\frac{z_{\alpha/2}}{E} \right]^2 \quad (6)$$

where $z_{\alpha/2}$ =value of the standard normal variate associated with a cumulative probability level, $(1 - \alpha/2)$. Let x be the number of true positive calls (hits) in M_{req} inspections. Eq. (6) implies that if (x/M_{req}) is used as an estimate for POD, we can assert with $100(1 - \alpha) \%$ confidence that the error will not exceed E .

Signal Response Method

This method is applied for inspection results recorded in terms of the parameter \hat{a} that indicates signal response to stimuli (cracks), such as the inspection results produced by ultrasonic inspection and eddy current inspection. For \hat{a} values below the recording signal threshold, \hat{a}_{th} , no signal is recorded. Also, \hat{a} values are displayed when they are greater than a specified decisive value, \hat{a}_{dec} ; however, for crack sizes that exceed the signal saturation limit, \hat{a}_{sat} , of the recording system, the corresponding \hat{a} values stay the same as \hat{a}_{sat} . Between \hat{a}_{th} and \hat{a}_{sat} , \hat{a} values can be related to the true crack size, a , as follows:

$$\ln \hat{a} = \beta_0 + \beta_1 \ln a + \varepsilon; \quad \hat{a}_{th} < a < \hat{a}_{sat} \quad (7)$$

where β_0 and β_1 =regression parameters; and ε =residual (assumed normally distributed) with a zero mean and a standard deviation, σ_ε associated with variability in the imperfect inspection procedure. As shown in Fig. 1, the probability of detection function, $POD(a)$, for a crack size a , can be expressed as

$$POD(a) = P[\hat{a}(a) \geq \hat{a}_{dec}] = \int_{\hat{a}_{dec}}^{\infty} f_{\hat{a}|a}(\hat{a}) d\hat{a} = 1 - F_{\hat{a}|a}(\hat{a}_{dec}) \quad (8)$$

where $f_{\hat{a}|a}(\hat{a})$ and $F_{\hat{a}|a}(\hat{a})$ =probability density function and the cumulative distribution function, respectively, of the signal value, \hat{a} , for a given crack of size a . Combining Eqs. (7) and (8), Berens (1989) suggested the POD function from the signal response method may be estimated as follows:

$$POD(a) = \Phi \left[\frac{\ln a - (\ln \hat{a}_{dec} - \beta_0)\beta_1}{\sigma_\varepsilon/\beta_1} \right] \quad (9)$$

where $\Phi(\cdot)$ =standard normal cumulative distribution function.

In this study, the POD function of each considered NDI technique with respect to the detail of interest reflects its capability. This POD function representing the corresponding NDI technique and other factors such as its cost will affect the optimal inspection procedure selected.

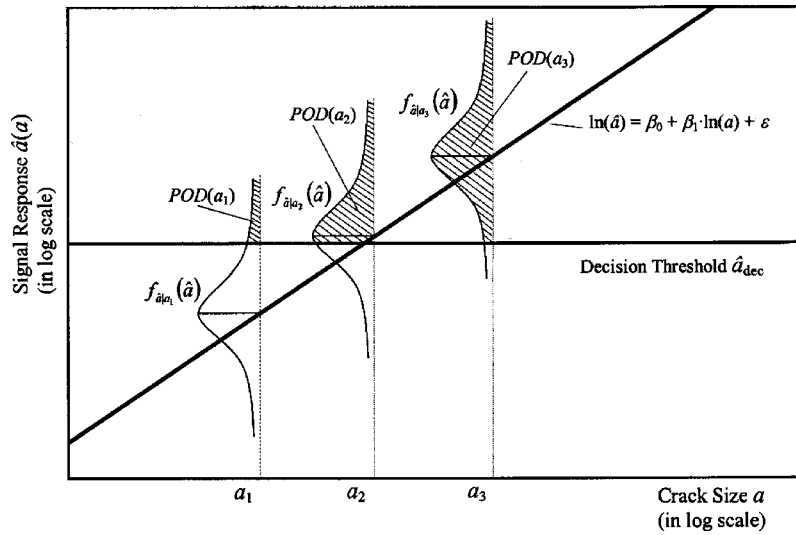


Fig. 1. Probability of detection function $POD(a)$ calculation in the signal response method (adapted from Berens 1989)

Fatigue Crack Growth Model

Following Paris and Erdogan (1963), the well-established linear elastic fracture mechanics (LEFM) procedure has been in use in many applications to relate crack growth to the number of stress cycles. An integral form of this relationship is

$$\int_{a_0}^{a_N} \frac{da}{[F(a)\sqrt{\pi a}]^m} = C \cdot N \cdot S_R^m \quad (10)$$

where a_0 =initial crack size; a_N =crack size after N stress cycles; $F(a)$ =geometry function; m =fatigue growth exponent; C =fatigue growth parameter; and S_R =stress range. If $\Psi(a)$ is defined as the indefinite integral form of the left side term of Eq. (10) when the crack reaches a size, a , this equation can be rewritten as

$$\Psi(a_N) - \Psi(a_0) = C \cdot N \cdot S_R^m \quad (11)$$

Note that, generally, the material properties (C and m) and initial crack size (a_0) are treated as random variables. The crack size, a_N , is then a function of the accumulated number of stress cycles (N) and the stress range (S_R) evaluated for the detail as follows:

$$a_N = \Psi^{-1}[\Psi(a_0) + C \cdot N \cdot S_R^m] \quad (12)$$

For structural details and components in a steel bridge, the main source of fatigue loading comes from vehicles, especially trucks, passing over the bridge. To account for the variable-amplitude stress ranges that result from random truck traffic, the stress range, S_R , in the crack growth model, is usually replaced by an effective stress range, S_{RE} , which represents a weighted effect of stress ranges of all amplitudes that occur in the detail. Based on Miner's rule (1945), for example, Schilling et al. (1978) proposed the use of the root mean cube (RMC) of the collected stress range spectrum in a detail as the effective stress range, S_{RE} , for fatigue evaluation

$$S_{RE} = \left(\sum_{i=1}^n \gamma_i \cdot S_{R,i}^3 \right)^{1/3} \quad (13)$$

where γ_i =ratio of the number of cycles with i th stress range amplitude, $S_{R,i}$, to the total number of cycles (a total of n ranges are considered). Furthermore, based on the analysis of 51 sets of

bridge stress range spectra from six sources including interstate and other routes in semirural and metropolitan locations, Schilling et al. (1978) showed that a Rayleigh distribution provides a reasonable model for the stress range spectrum of details in steel bridges. The probability density function for the stress range, S_R , can be expressed as

$$f_{S_R}(s) = \left(\frac{s}{S_{R0}} \right) \cdot \exp \left[-\frac{1}{2} \left(\frac{s}{S_{R0}} \right)^2 \right]; \quad \text{where } S_{R0} = \sqrt{\frac{2}{\pi}} \cdot E[S_R] \quad (14)$$

where $E[S_R]$ =mean value of S_R , while S_{R0} =stress value related to $E[S_R]$ as well as to the effective stress range, S_{RE} , which for a Rayleigh distribution analysis is easily expressed in terms of the gamma function, $\Gamma(\cdot)$, as follows:

$$S_{RE} = \{E[S_R^m]\}^{1/m} = \sqrt{2} S_{R0} \cdot \Gamma \left(\frac{m}{2} + 1 \right)^{1/m} \quad (15)$$

The geometry function, $F(a)$, for a specific fatigue detail in a steel bridge may be obtained from available stress intensity manuals or derived using fracture mechanics principles. Table 2 shows a few common geometry functions that may be applied in box girder steel bridges.

The number of stress cycles (N) after N years in service (Y) is computed as

$$N = C_S \cdot (365 \cdot \text{ADTT} \cdot Y) \quad (16)$$

where C_S =number of stress cycles per truck passage; and ADTT=average daily truck traffic crossing the bridge.

Eqs. (12) and (16) together permit estimation of the crack growth as a function of the number of years, Y , in service. As a special case, when $F(a)$ is taken to be unity, one obtains (see Madsen et al. 1985)

$$a(Y) = \left[a_0^{(2-m)/2} + \frac{2-m}{2} \cdot \pi^{m/2} \cdot C \cdot S_{RE}^m \cdot (365 \cdot \text{ADTT} \cdot C_S \cdot Y) \right]^{2/(2-m)} \quad (17)$$

for $m \neq 2$

Table 2. Fatigue Geometry Functions for Some Common Details in Steel Bridges

Crack pattern	Geometry function $F(a)$
Center-notched crack in flange	$F(a) = [1 - 0.025(a/b)^2 + 0.06(a/b)^4] \cdot \sqrt{\sec \frac{\pi a}{2b}}$
Single-edged crack in flange	$F(a) = \sqrt{\frac{2b}{\pi a} \tan \frac{\pi a}{2b}} \cdot \left[\frac{0.752 + 0.02(a/b) + 0.37 \left(1 - \sin \frac{\pi a}{2b}\right)^3}{\cos \frac{\pi a}{2b}} \right]$
Distributed cracks in flange	$F(a) = \left[\frac{2b}{\pi a} \tan \left(\frac{\pi a}{2b} \right) \right]^{0.5}$

$$a(Y) = a_0 \cdot \exp[\pi \cdot C \cdot S_{RE}^2 \cdot (365 \cdot ADTT \cdot C_S \cdot Y)] \quad \text{for } m = 2 \quad (18)$$

According to LEFM principles, fracture results when the stress intensity factor, K , associated with a crack exceeds the fracture toughness, K_c , of the material. In other words, the crack growth relations in Eqs. (12), (17), and (18) are valid only as long as the crack size remains smaller than the critical crack size, a_{cr} , associated with K_c .

Simulation of Crack Propagation and Inspection Scenarios

Consider a situation where n nondestructive fatigue inspections are performed on a fracture-critical member of a steel bridge at fixed points in time, y_1, y_2, \dots, y_n . In each possible crack growth curve realization, the crack in the detail is assumed to reach its critical crack size at a time, y_{cr} [i.e., $a(y_{cr}) = a_{cr}$]. By applying a crack growth model, the size, a_i , of the crack at each inspection time, y_i , can be estimated. By mapping each such crack size, a_i , onto the POD curve for the chosen NDI technique, the probability of detecting the crack size, a_i , denoted as p_i , can be estimated. This mapping procedure is shown schematically in Fig. 2. Therefore, the probability of not detecting a crack, P_{nd} , and the probability of detecting a crack, P_d , before fracture occurs can be expressed as

$$P_{nd} = \prod_{i=1}^n (1 - p_i) \quad (19)$$

$$P_d = 1 - P_{nd} = 1 - \prod_{i=1}^n (1 - p_i) \quad (20)$$

where n = number of inspections before the critical crack size, a_{cr} , is reached. Fixed-interval inspection schedules are considered in this study in order to conform with practical application for bridges. If the inspection interval, y_{int} , and the time to fracture, y_{cr} , are known, the value of n can be obtained without difficulty.

The initial crack size (a_0), material properties (C and m) for the detail, and traffic-related quantities ($ADTT$, C_S , and S_{RE}) are taken as random variables with specified probability distributions. Individual crack growth realizations arising from Monte Carlo simulations with these random variables yield curves such as are shown in Fig. 3. For a specified inspection interval, each crack growth simulation, i , provides two quantities of interest: (1) the probability that a crack is not detected before fracture results,

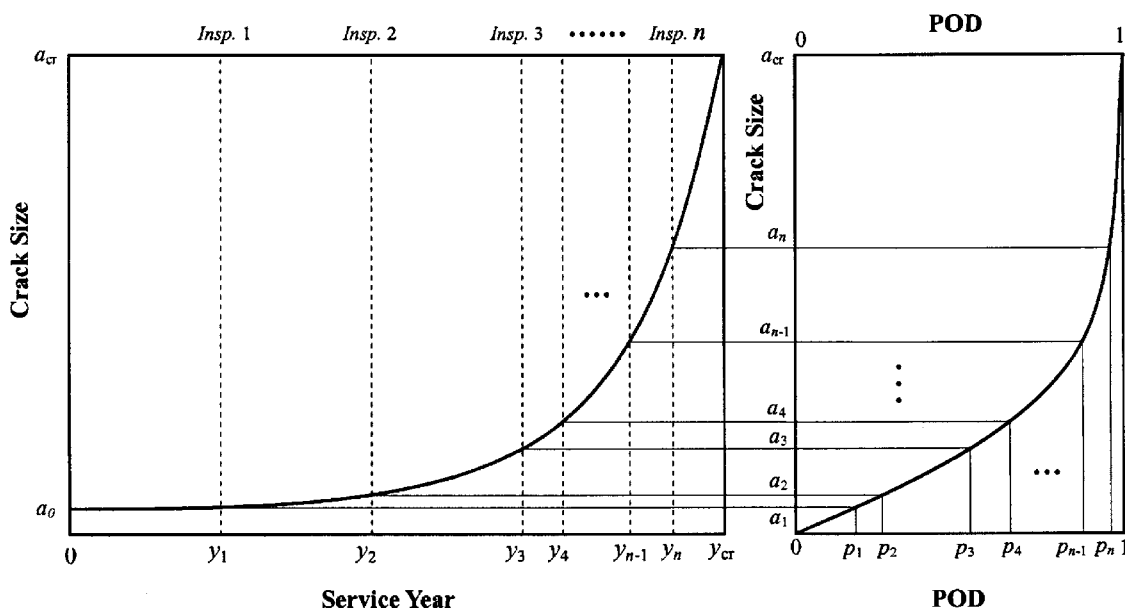


Fig. 2. Mapping of crack size with probability of detection and time in service

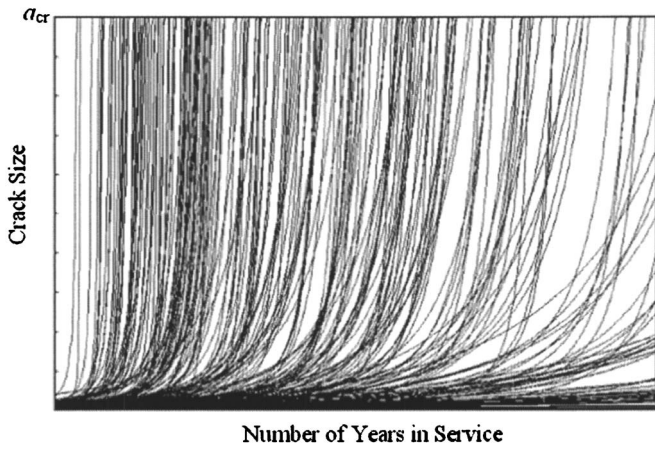


Fig. 3. Monte Carlo simulations of crack growth curves

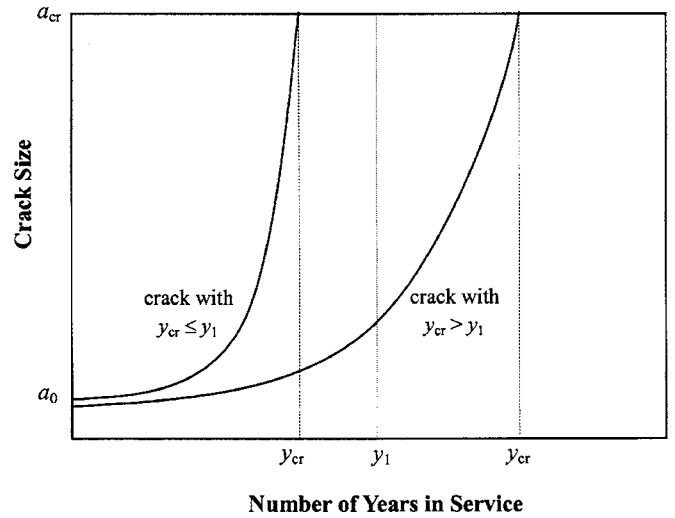


Fig. 4. Crack growth curves for $y_{cr} \leq y_1$ and $y_{cr} > y_1$

$P_{nd,i}$; and (2) the number of inspections, n_i , before fracture. Using the results of all the crack growth N_{sim} simulations, the expected probability of not detecting a crack, $E[P_{nd}]$, before fracture, and the expected number of inspections, $E[n]$, before fracture can be obtained as follows:

$$E[P_{nd}] = \frac{1}{N_{sim}} \sum_{i=1}^{N_{sim}} P_{nd,i} \quad (21)$$

$$E[n] = \frac{1}{N_{sim}} \sum_{i=1}^{N_{sim}} n_i \quad (22)$$

By employing a sufficiently large number of simulations, converged estimates of $E[P_{nd}]$ and $E[n]$ can be obtained. For the given POD curve associated with the selected NDI technique and for the selected inspection schedule, $E[P_{nd}]$ represents the risk of failure to detect an existing crack in a detail before fracture occurs. Also, $E[n]$ represents the expected number of inspections performed during the fatigue life of the detail (i.e., before fracture occurs). It should be noted that the crack growth simulations here do not account for any repair activity.

Because the crack growth curves are simulated randomly by the Monte Carlo method, the time to failure, y_{cr} , in a single simulation may be either longer or shorter than the time, y_1 , when the first inspection is performed, as shown in Fig. 4. For simulations with detail lives longer than the first inspection time, instead of using Eqs. (21) and (22), the expected probability of not detecting a crack and the expected number of inspections before fracture may be computed as follows:

$$\begin{aligned} E[P_{nd}] &= E[P_{nd}|y_{cr} \geq y_1] \cdot P(y_{cr} \geq y_1) \\ &\quad + E[P_{nd}|y_{cr} < y_1] \cdot P(y_{cr} < y_1) \\ &= \left(\frac{\sum_{i=1}^{N_1} P_{nd,i}}{N_1} \right) \cdot \left(\frac{N_1}{N_{sim}} \right) + \left(\frac{1 \cdot N_2}{N_2} \right) \cdot \left(\frac{N_2}{N_{sim}} \right) \\ &= \frac{\sum_{i=1}^{N_1} \left[\prod_{j=1}^{n_i} (1 - p_j) \right] + N_2}{N_{sim}} \end{aligned} \quad (23)$$

$$\begin{aligned} E[n] &= E[n|y_{cr} \geq y_1] \cdot P(y_{cr} \geq y_1) + E[n|y_{cr} < y_1] \cdot P(y_{cr} < y_1) \\ &= \left(\frac{\sum_{i=1}^{N_1} n_i}{N_1} \right) \cdot \left(\frac{N_1}{N_{sim}} \right) + (0) \cdot \left(\frac{N_2}{N_{sim}} \right) = \frac{\sum_{i=1}^{N_1} n_i}{N_{sim}} \end{aligned} \quad (24)$$

where N_1 = number of simulations for which $y_{cr} \geq y_1$; N_2 = number of simulations for which $y_{cr} < y_1$; $N_{sim} (= N_1 + N_2)$ = total number of simulations; and n_i = number of inspections in the i th simulation prior to fracture. Note that for simulations where the fatigue life is shorter than the time until the first inspection, the probability of not detecting a crack is 1, since no inspections will have been performed before a_{cr} is reached. A schematic outline of the Monte Carlo simulations and associated computations of $E[P_{nd}]$ and $E[n]$ is presented in Fig. 5.

Optimal Nondestructive Inspection Technique and Schedule

Practical challenges for bridge inspectors include the need to come up with answers to questions such as “What kind of NDI technique should I use and how often should I perform the inspections?” At present in the United States, fracture-critical inspections for structural members in steel bridges either follow the FHWA’s two-year interval requirement, or sometimes an annual inspection plan in some states based on the judgment of the responsible engineer. However, each steel bridge has its own specific geometric configuration, design philosophy, and traffic conditions, and even on the same bridge, details may have different expected fatigue performance and will experience quite different levels of stress ranges. These different fatigue performance expectations and stress ranges result in different fatigue lives for each detail. Hence, an ad hoc fixed inspection interval program might not meet the safety demands for all types of fatigue details on steel bridges. A rational method for selecting a suitable NDI technique and inspection frequency can be useful. A probabilistic method is proposed here that employs LEFM-based fatigue analysis, actual NDI technique detectabilities, and Monte Carlo simulations leading to the selection of an optimal

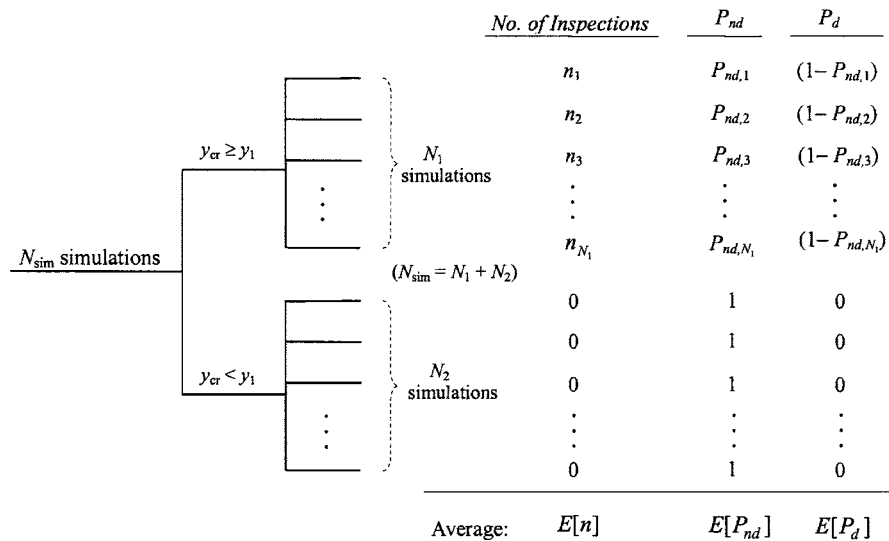


Fig. 5. Monte Carlo simulation scenarios and associated computations

NDI technique and associated inspection schedule for fracture-critical members in steel bridges. The procedure is formulated so as to yield a balanced solution that takes into consideration both economy and safety.

Cost Function

In order to represent the problem of selection of a proper NDI technique as an optimization problem, a cost function must be defined that accounts for the consequences of choosing an NDI technique and associated inspection schedule for the detail or member under consideration. Together with the expected number of inspections, $E[n]$, and the expected probability of not detecting a crack, $E[P_{nd}]$, for any NDI technique and inspection schedule, a cost function including the cost of inspections and the expected cost of failure can be assembled.

Cost of Inspections

From the Monte Carlo simulations, $E[n]$ represents the expected number of inspections of the specified detail (prior to failure) for a specified NDI technique and associated inspection schedule. If K_I denotes the cost of a single such inspection, the expected total cost of inspections over the service life, C_I , can be computed as

$$C_I = K_I \cdot E[n] \quad (25)$$

Cost of Failure

From the Monte Carlo simulations, $E[P_{nd}]$ represents the expected probability of not detecting a crack in the specified detail or member (prior to failure) with the chosen NDI technique and schedule. If, in the simulations, an NDI technique often fails to detect a growing crack in the detail, the associated expected fatigue failure probability will be high. Clearly, $E[P_{nd}]$ provides an indication of the likelihood of fatigue failure of the detail as a result of failure to detect a growing crack with the NDI technique and associated inspection schedule. The risk of fatigue failure for the specified detail can be represented by an estimate of the (expected) cost of failure, C_F . If the detail/member under consideration is fracture-critical, its failure could cause failure of the

span where the detail is located or even failure of the entire bridge. Hence, the cost of failure might include the possible cost of rebuilding a span or the entire bridge, as appropriate, as well as costs due to lost use, injuries, fatalities, etc.—not all of these costs are easily and uncontroversially estimated. Nevertheless, all of these potential costs are included in K_F , the cost associated with a failure. The likelihood of such failures is the other term needed to arrive at the expected cost of failure, C_F , which for the specified member or detail may then be defined as

$$C_F = K_F \cdot E[P_{nd}] \quad (26)$$

Total Cost

Using the definitions of the cost of inspections and failure in Eqs. (25) and (26) that result from selection of an NDI technique and its associated inspection schedule, the total cost, C_T , may be represented as

$$C_T = C_I + C_F \quad (27)$$

$$C_T = K_I \cdot E[n] + K_F \cdot E[P_{nd}] \quad (28)$$

Optimization Variables

The POD function corresponding to an NDI technique and the fixed interval, y_{int} , employed in an inspection program are the optimization variables in our optimization problem. The reason for employing a fixed-interval inspection schedule here is to conform to the practical realities of bridge inspections. The POD function for the chosen NDI technique directly affects the value of $E[P_{nd}]$ and the inspection interval, y_{int} , affects both $E[n]$ and $E[P_{nd}]$. Clearly then, the total cost defined in Eq. (28) is influenced by the POD function and the inspection interval, y_{int} , in a direct manner. By varying the POD function (or, effectively by choosing a different NDI technique) and the inspection interval, y_{int} , an optimal combination of the two can be found that yields the minimum cost.

Constraints

A target probability level, $P_{nd,max}$, defined as the maximum allowable probability of not detecting a crack (or the minimum acceptable safety level) for an NDI technique applied on a specified fatigue detail is employed as a constraint in order to exclude combinations of NDI techniques and inspection schedules that might be deemed unsafe because $E[P_{nd}]$ is too high. This constraint can be expressed as

$$E[P_{nd}] < P_{nd,max} \quad (29)$$

Additionally, restrictions are placed on the time between inspections so that this inspection interval is neither too large (upper bound, y_{max}) nor too short (lower bound, y_{min}). Such constraints on the inspection interval may be required by local or state transportation agencies. Hence, a second constraint on the inspection interval for the optimization problem is

$$y_{min} < y_{int} < y_{max} \quad (30)$$

Formulation of the Optimization Problem

In summary, the optimization problem for the selection of an optimal NDI technique and associated inspection schedule may be formulated as follows:

$$\min_{POD, y_{int}} C_T = K_I \cdot E[n] + K_F \cdot E[P_{nd}]$$

optimization variables: POD function and inspection interval, y_{int}

$$\text{subject to: } E[P_{nd}] < P_{nd,max}; \quad y_{min} < y_{int} < y_{max}. \quad (31)$$

For a given NDI technique (or POD function), an optimum inspection interval, y_{int} , can be found. In addition, by considering alternate NDI techniques, the total cost corresponding to the alternate POD functions can be compared so as to finally yield the optimal choice of NDI technique and associated inspection schedule.

To solve the optimization problem, the Monte Carlo method is employed to estimate the expected probability of not detecting a crack, $E[P_{nd}]$, and the expected number of inspections, $E[n]$, prior to failure for a given NDI technique and an associated inspection schedule by treating the initial crack size (a_0), crack growth parameter (C), and crack growth exponent (m) as random variables. After $E[P_{nd}]$ and $E[n]$ are estimated, the total cost for the given NDI technique and associated schedule can be evaluated. By changing the NDI technique and inspection schedule, repeated computations of total cost are obtained. The optimal choice comes from the NDI technique and schedule that lead to the minimum total cost. A flow chart describing this procedure is presented in Fig. 6.

Numerical Example

Two full-penetration butt welds in the bottom (tension) flange of a newly built steel box girder bridge are studied in this example, for which we seek an optimal NDI technique and inspection schedule. It is assumed that failure of the butt weld detail will result in collapse of the box-girder span. An inherent flaw is assumed to exist in the butt welds of the 1.52 m (60 in.) width (w) bottom flange as shown in Fig. 7. The initial flaw size, a_0 , is modeled as a lognormally distributed random variable with a mean value of 0.508 mm (0.02 in.) and a coefficient of variation

of 0.5. The critical crack size, a_{cr} , is considered to be constant at 50.8 mm (2 in.) for this example. The fatigue growth parameter, C , is modeled as a lognormal variable with a mean value of 2.18×10^{-13} assuming units of millimeters for crack size and $\text{Mpa} \cdot \text{m}^{1/2}$ for fracture toughness (or, equivalently, 2.05×10^{-10} , assuming units of inches for crack size and $\text{ksi} \cdot \text{in}^{1/2}$ for fracture toughness) and a coefficient of variation of 0.63. The fatigue growth exponent, m , is modeled as a normally distributed random variable with a mean value of 3.0 and a coefficient of variation of 0.1. The average daily truck traffic, ADTT, and the number of stress cycles per truck passage, C_s , for the box girder bridge are taken to be 600 and 1.0, respectively. A Rayleigh distribution with S_{R0} equal to 43.67 MPa (6.334 ksi) is employed to model the stress range spectrum for the bottom flange of the bridge.

Three NDI techniques—UI, MI, and PI—are considered here for the butt weld detail. The POD functions for these three techniques, based on POD data from flat plate testing results collected by Rummel and Matzkanin (1997), are presented in Fig. 8. In practice, the POD functions for these three NDI techniques would need to be obtained from numerous tests of similar butt weld details because POD functions depend on the actual test object (form and material), the anomaly condition, the NDI procedure, and the operator, as was observed by Rummel (1998). The three illustrative POD functions are presented in Table 3. Two cases of relative costs for the three types of NDIs and of the cost of failure are considered here: (1) $K_{I,PI}:K_{I,MI}:K_{I,UI}:K_F=1.0:1.2:1.5:2.0 \times 10^4$; and (2) $K_{I,PI}:K_{I,MI}:K_{I,UI}:K_F=1.0:1.2:1.5:4.0 \times 10^4$. The maximum acceptable probability of not detecting a crack over the service life is taken to be 0.005 (i.e., $E[P_{nd}] < 0.005$, or $P_{nd,max}=0.005$) in this example.

Because the initial crack size, a_0 , is relatively small compared to the width of the bottom flange, w (i.e., $a_0/w \approx 3.3 \times 10^{-4}$), the geometry function $F(a)$ is taken to be unity for simplicity to model the stress intensity factor for the crack. Hence, Eqs. (17) and (18) can be employed here to predict crack growth rates here. Fig. 9 shows the probability density function for the fatigue life, Y_{cr} , of the detail under consideration.

For the detail under consideration, five million Monte Carlo simulations are carried out in order to achieve stable results for the first case of the relative costs of the three NDIs and failure, namely— $K_{I,PI}:K_{I,MI}:K_{I,UI}:K_F=1.0:1.2:1.5:2.0 \times 10^4$. Fig. 10 shows 350 such simulated crack growth curves.

Figs. 11–13 show costs for various fixed-interval schedules of UIs, MIs, and DIs, respectively. In these figures, each value of y_{int} on the abscissa represents a schedule that employs y_{int} as the inspection interval for the detail under consideration over the service life. Expectedly, the three figures show a tendency for longer inspections intervals to be associated with lower expected costs of inspections, C_I , but higher expected costs of failure, C_F . On the other hand, schedules with shorter inspection intervals have higher expected costs of inspections, C_I , but lower expected costs of failure, C_F ; the higher inspection costs result due to the increased number of inspections expected with a shorter inspection interval, while the lower expected failure costs result due to the smaller likelihood of failing to detect a crack before fracture occurs. The combined effect of the opposing trends in C_I and C_F with length of inspection interval helps to yield a solution with lowest total cost, $C_{T,min}$, and an optimal inspection schedule, $y_{int,opt}$, for each NDI technique as is shown in the three figures. Before comparing the optimal inspection intervals and costs for the three NDI techniques, the constraint $E[P_{nd}] < 0.005$ needs to be verified first to eliminate any infeasible schedules. As shown in Fig. 14, for the ultrasonic inspection, feasible schedules are only

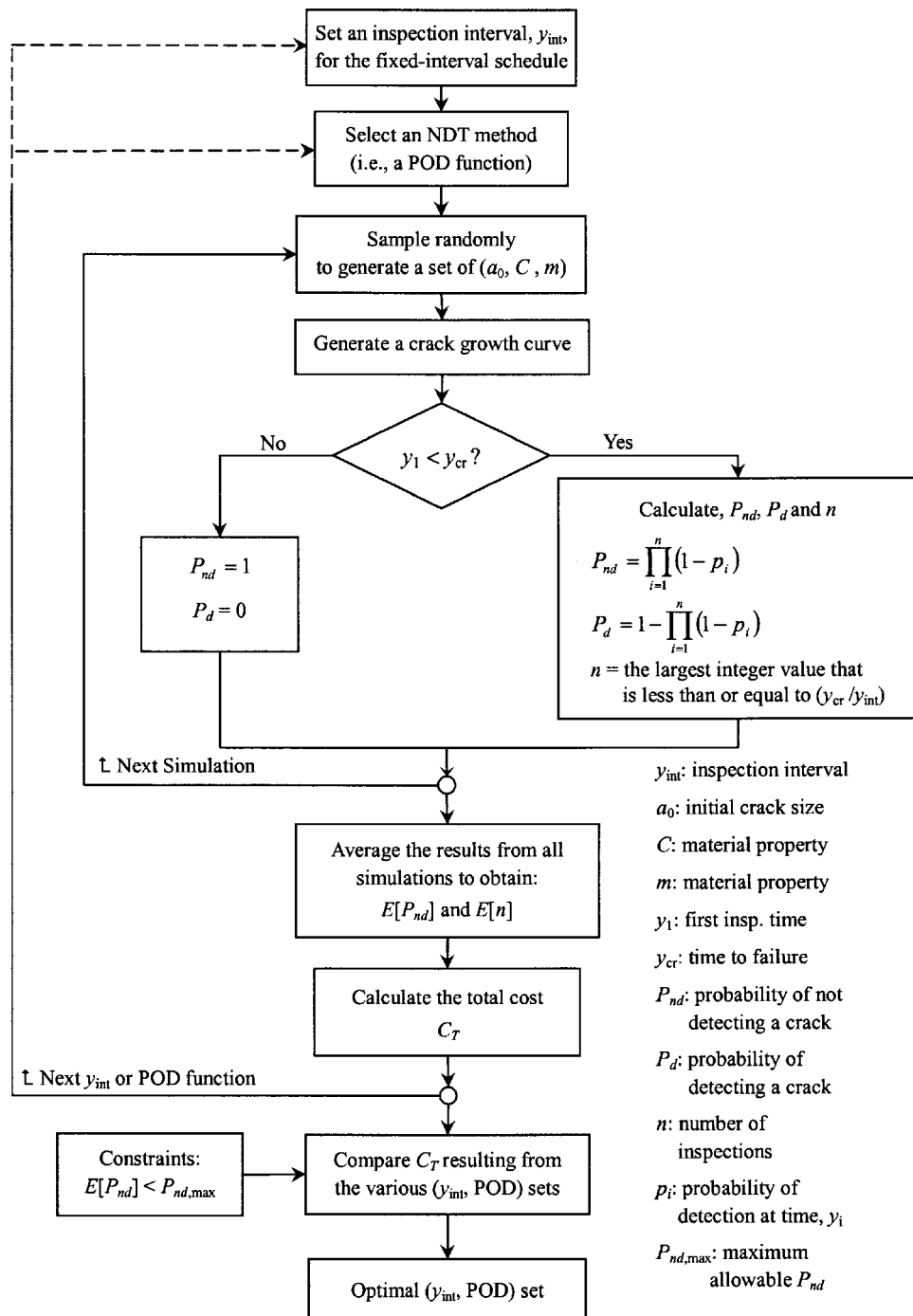


Fig. 6. Flow chart of the optimization procedure

those where the fixed inspection interval is less than or equal to five years. Likewise, for magnetic particle and penetrant inspections, the maximum feasible inspection intervals are four and two years, respectively. After eliminating infeasible schedules, the optimal schedule with the ultrasonic method involves performing inspections every three years and leads to a total cost of 63.9 (see Fig. 11). For magnetic particle inspections, the optimal schedule involves inspections every 2.5 years and a total cost of 66.1 (see Fig. 12). Finally, for penetrant inspections, the optimal schedule involves inspections every 1.5 years and a total cost of 95.4 (see Fig. 13). Combining Figs. 11–13 and the

constraint on $E[P_{nd}]$, Fig. 15 shows total costs for various fixed-interval inspection schedules with the three NDI techniques. Note that each marker “×” in Fig. 15 indicates an infeasible schedule that fails to meet the constraint $E[P_{nd}] < 0.005$. It can be seen that if all three NDI techniques are candidates for inspection of the detail in question, the overall optimal plan would suggest carrying out ultrasonic inspections every three years. As summarized in Table 4, even though a single ultrasonic inspection is more expensive than a single magnetic particle or penetrant inspection ($K_{I,PT}:K_{I,MT}:K_{I,UT}:K_F=1.0:1.2:1.5$), the less frequent inspections and higher flaw detectability of the UI technique together yield

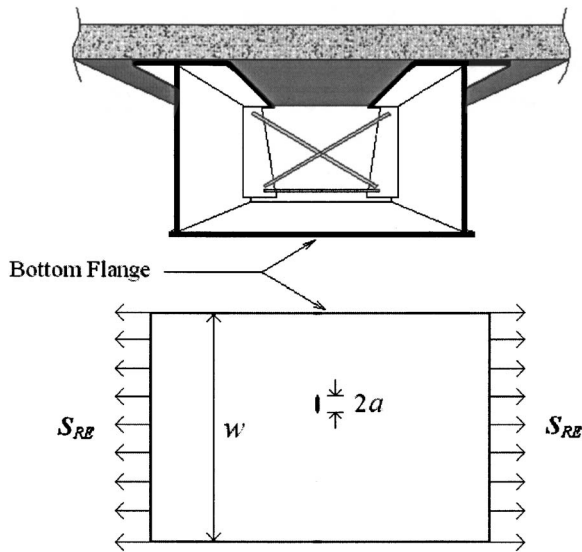


Fig. 7. Detail in a fracture-critical member of the box girder bridge

lower total costs than those resulting from use of the other two NDI techniques. Both magnetic particle and penetrant inspections have lower single-inspection costs, but the greater number of inspections and the higher probability of failure to detect a crack (before fracture) resulting from a lower flaw detectability lead to higher total costs than with ultrasonic inspections.

The constraint, $P_{nd,max}=0.005$ (i.e., $E[P_{nd}]<0.005$), eliminates some infeasible inspection schedules, typically those with long inspection intervals. A relatively larger number of schedules are eliminated for an NDI technique that has low detectability, such as PI. From Fig. 15, it can be seen that the optimal schedule for each NDI technique (when $P_{nd,max}$ is 0.005) can be directly identified from the local minima of the three cost curves so that the $P_{nd,max}$ constraint virtually does not affect the optimization solution in this case. However, when a stricter constraint, $P_{nd,max}=0.001$ (i.e., $E[P_{nd}]<0.001$), is enforced, a greater number

Table 3. POD Functions for Penetrant, Magnetic Particle, and Ultrasonic Inspections

NDI technique	POD(a) = $\frac{\exp[\alpha + \beta \cdot \ln a]}{1 + \exp[\alpha + \beta \cdot \ln a]}$	
	α	β
UI	-0.119	2.986
MI	0.466	0.604
PI	-0.561	0.393

Note: The form of the POD model used is proposed by Berens and Hovey (1981). The parameters α and β are estimated using the maximum likelihood method (units of a : mm).

of schedules become infeasible as can be seen in Fig. 16. The optimal inspection interval for PI, for example, changes from 1.5 years ($C_T=95.3$) to one year ($C_T=104.6$), and for MI, it changes from 2.5 years ($C_T=66.1$) to two years ($C_T=67.0$). Both these NDI methods demand more frequent inspections to satisfy the stricter $P_{nd,max}$ constraint which, therefore, results in higher total costs. Note that the three-year inspection interval schedule yielding the minimum total cost ($C_T=63.9$) for ultrasonic inspections met the original $P_{nd,max}=0.005$ constraint as well as the stricter $P_{nd,max}=0.001$ constraint; as a result, the optimal UI schedule is unchanged.

For the higher relative failure cost case where $K_{I,PT}:K_{I,MT}:K_{I,UT}:K_F=1.0:1.2:1.5:4.0 \times 10^4$ and with the constraint, $P_{nd,max}=0.005$, the $E[n]$ and $E[P_{nd}]$ values from the Monte Carlo simulations remain the same as in the lower failure cost case; but the higher relative failure cost, K_F , raises the failure cost curve twice as much as before. This results in higher total costs for each of the three NDI techniques, especially for those schedules with large $E[P_{nd}]$ values (see Figs. 17–19). Compared to the lower relative failure cost case, for each NDI technique, the higher total cost curve now shifts the schedule with the minimum cost to one with shorter inspection intervals. Comparing Figs. 15 and 20, the schedule with the minimum total cost for UI changes from a three-year inspection interval (with $C_T=63.9$) to a 2.5-year inter-

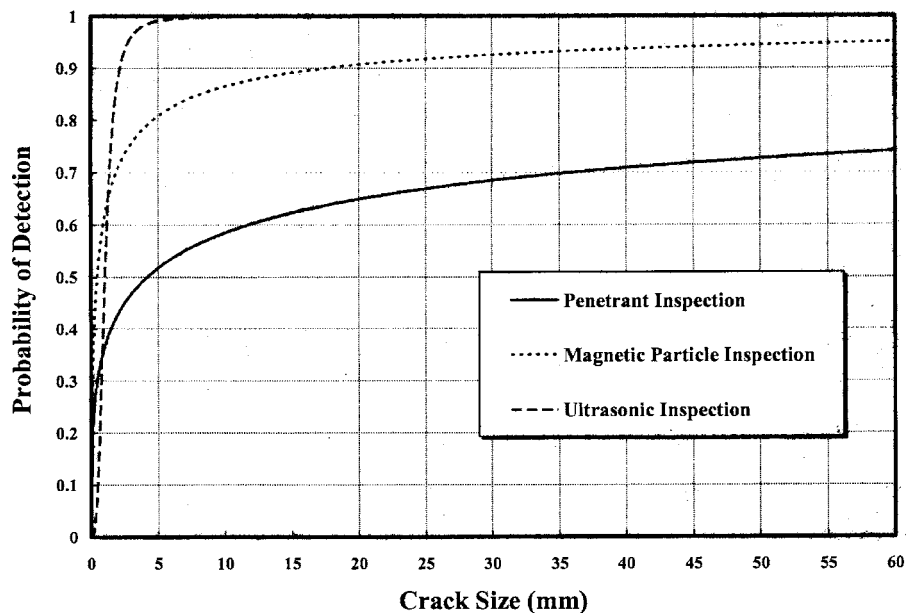


Fig. 8. Probability of detection curves for penetrant, magnetic particle, and ultrasonic inspections

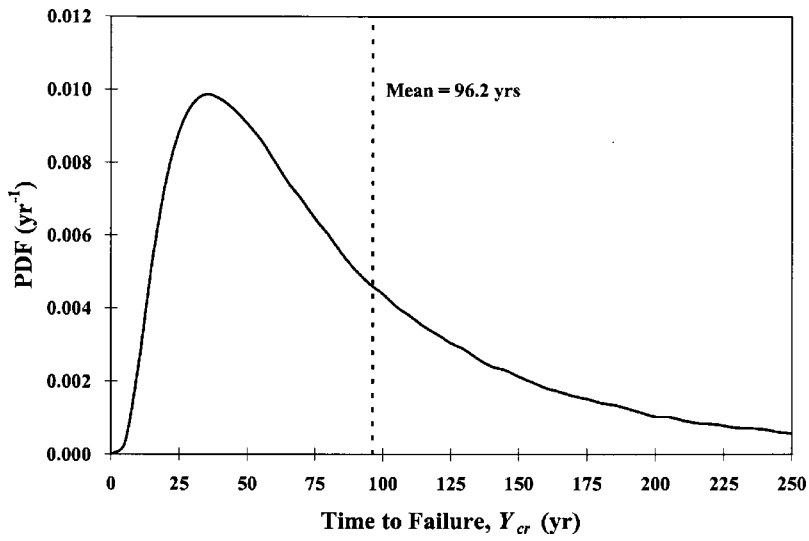


Fig. 9. Probability density function of the time to failure, Y_{cr}

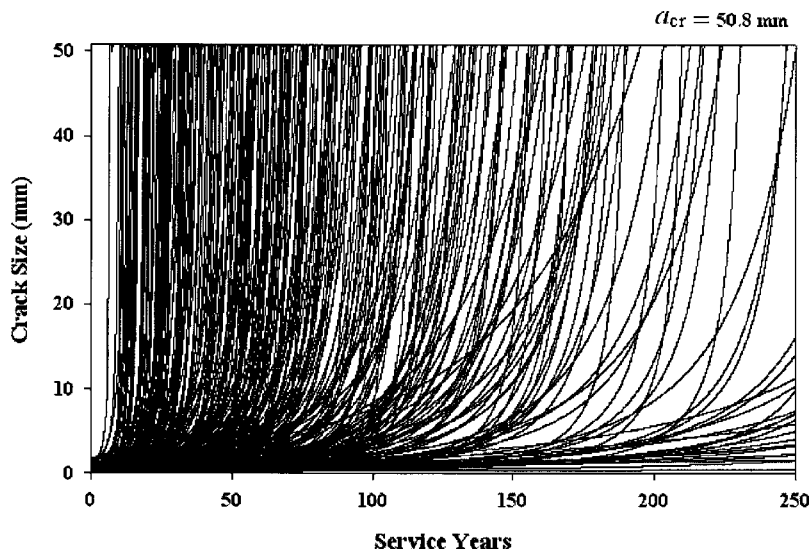


Fig. 10. Three hundred and fifty crack growth simulations [$a_{cr} = 50.8$ mm (2 in.)]

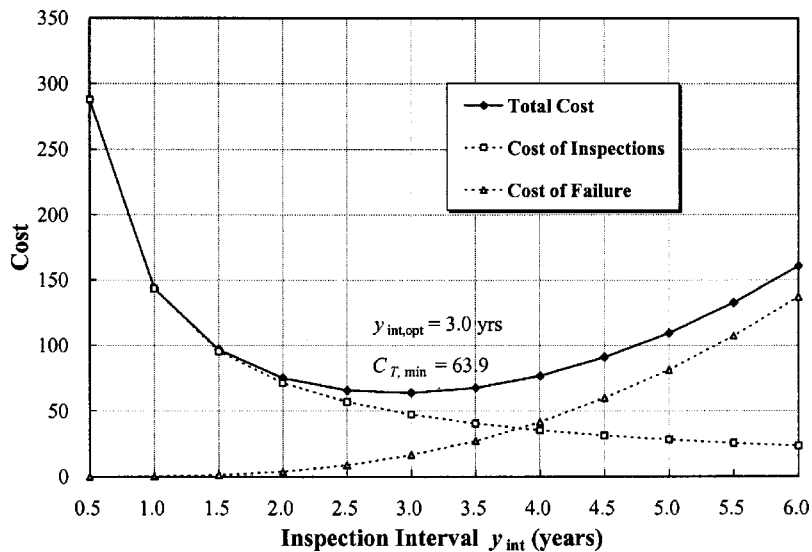


Fig. 11. Costs of ultrasonic inspections for various fixed-interval schedules for $K_{I,UI}:K_F = 1.5:2 \times 10^4$

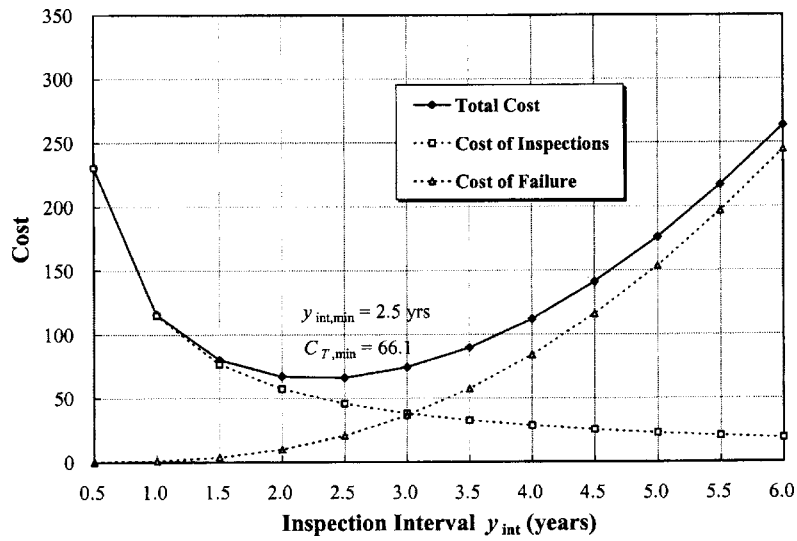


Fig. 12. Costs of magnetic particle inspections for various fixed-interval schedules for $K_{I,MI}:K_F=1.2:2 \times 10^4$

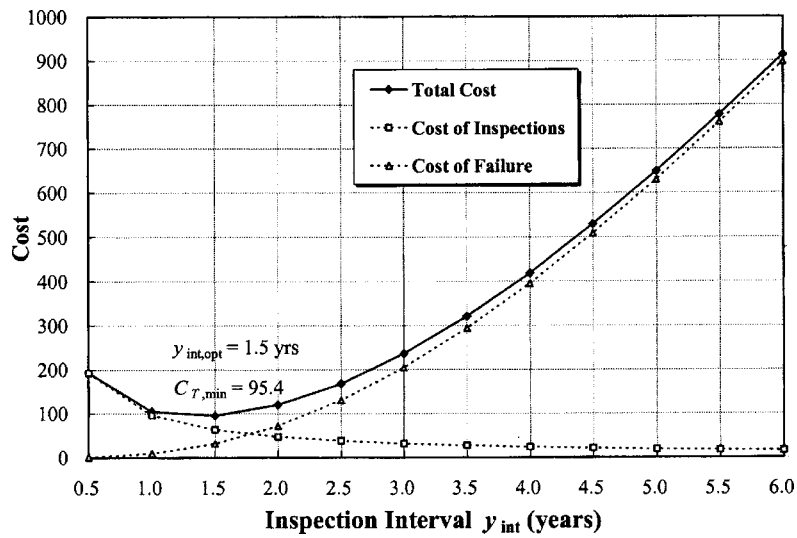


Fig. 13. Costs of penetrant inspections for various fixed-interval schedules for $K_{I,PI}:K_F=1.0:2 \times 10^4$

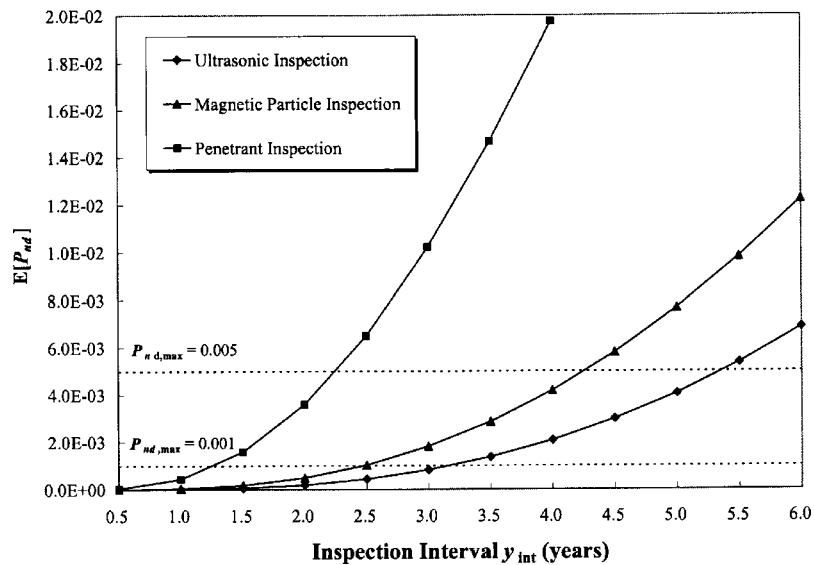


Fig. 14. Expected probabilities of failure to detect a growing crack before fracture, $E[P_{nd}]$, for the UI, MI, and PI techniques compared with the maximum acceptable probability of nondetection, P_{nd}

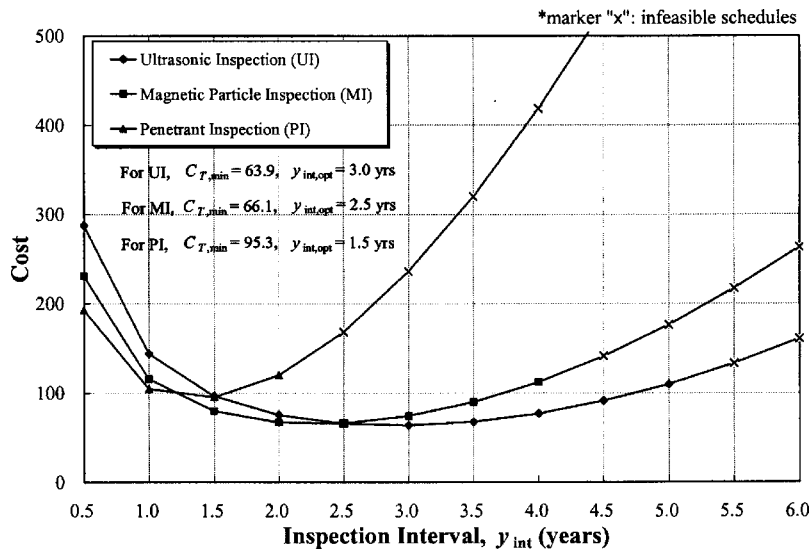


Fig. 15. Cost comparison of UI, MI, and PI in various fixed-interval schedules for $K_{I,PI}:K_{I,MI}:K_{I,UI}:K_F=1.0:1.2:1.5:2 \times 10^4$ (showing infeasible schedules when $P_{nd,max}=0.005$)

val (with $C_T=74.5$). The three-year periodic schedule in the higher failure cost case has a total cost of 80.4 for UI and is thus no longer the best schedule. For MI, the schedule changes from a 2.5-year inspection interval (with $C_T=66.1$) to a two-year interval (with $C_T=76.8$); and, for PI, the schedule changes from a 1.5-year inspection interval (with $C_T=95.3$) to a one-year interval (with $C_T=113.4$).

If all three NDI techniques are considered candidates for inspection of the detail in question, the overall optimal plan in this higher failure cost case recommends carrying out ultrasonic inspections every 2.5 years. This is to be contrasted with the three-year periodic UI schedule found before. Total costs will be a little higher than before. Thus, increases in the relative failure cost, K_F , affect the optimization solution in a direct manner. In the procedure outlined, higher K_F values tend to yield an optimal strategy that demands more frequent inspections and higher NDI detectability. This is evident from the optimization results and is consistent with the expectation that more important details or members (associated with higher failure costs or consequences) should require more frequent and precise inspections.

The original $E[P_{nd}]$ values (shown in Fig. 14) for all schedules with the three NDI techniques remain unaffected when higher relative failure costs are considered. Hence, the infeasible schedules under a stricter constraint, $P_{nd,max}=0.001$, remain the same as in the lower relative failure cost case with the same $P_{nd,max}$ constraint (compare Figs. 21 and 16). The schedules for UI, MI, and PI with inspection intervals greater than and equal to 3.5 years, 2.5 years, and 1.5 years, respectively, are identified as infeasible. It can be confirmed from Fig. 21 that the stricter constraint, $P_{nd,max}=0.001$, does not change the schedule with

minimum total cost for each NDI technique so that the optimal strategy is still to carry out ultrasonic inspections every 2.5 years.

Results from the two cases discussed have shown that any ad hoc periodic inspection schedule (annual or biennial, for example) without consideration for the quality of inspection may not lead to the optimal schedule for a butt weld detail inspected by any of the three NDI techniques studied here. Besides, if costs are included, useful insights may be gained to guide selection of the optimal inspection strategy using the optimization procedure presented.

Conclusions

A probabilistic approach for selecting an optimal NDI technique and an associated inspection schedule for fracture-critical members in steel bridges has been presented. The method builds upon LEFM principles and detection capabilities of NDI techniques for the fracture-critical member or detail of interest, and then employs the probability of detection information in Monte Carlo simulations to formulate an optimization problem. Solution of this problem yields the optimal NDI technique and associated inspection schedule for the detail and takes into consideration safety and economy. Based on the numerical examples, some key findings are summarized as follows:

1. For a given NDI technique, the total cost is controlled by the cost of inspections for schedules with short inspection intervals. This is because the shorter the inspection interval employed, the greater will be the cost of inspections toward total cost. For schedules with longer inspection intervals, the total cost is governed more by the cost of failure than by inspection costs. Also, the longer the fixed inspection interval, the greater will be the possibility of failure to detect a crack; this leads to higher failure costs. A valley-shaped total cost versus inspection interval curve results. After applying a constraint on minimum acceptable safety, some infeasible schedules are eliminated and the optimal schedule for an NDI technique is often found at the bottom of the valley-shaped total cost curve.

Table 4. Optimization Results for the Ultrasonic, Magnetic Particle, and Penetrant Inspection Techniques with the Constraint $P_{nd,max}=0.005$

NDI technique	$E[n]$	$E[P_{nd}]$	$y_{int,opt}$ (years)	$C_{T,min}$
Ultrasonic	31.2	8.26×10^{-4}	3.0	63.9
Magnetic Particle	38.0	1.02×10^{-3}	2.5	66.1
Penetrant	63.6	1.59×10^{-3}	1.5	95.3

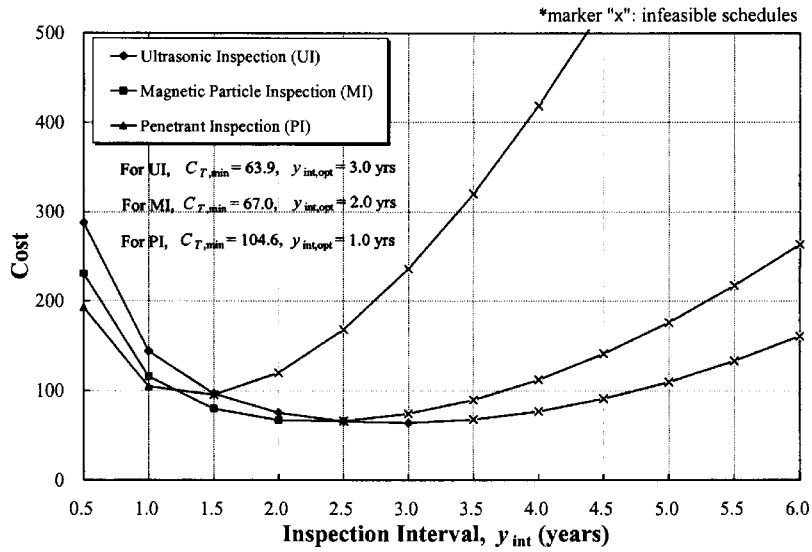


Fig. 16. Cost comparison of UI, MI, and PI in various fixed-interval schedules for $K_{I,PI}:K_{I,MI}:K_{I,UI}:K_F=1.0:1.2:1.5:2 \times 10^4$ (showing infeasible schedules when $P_{nd\ max}=0.001$)

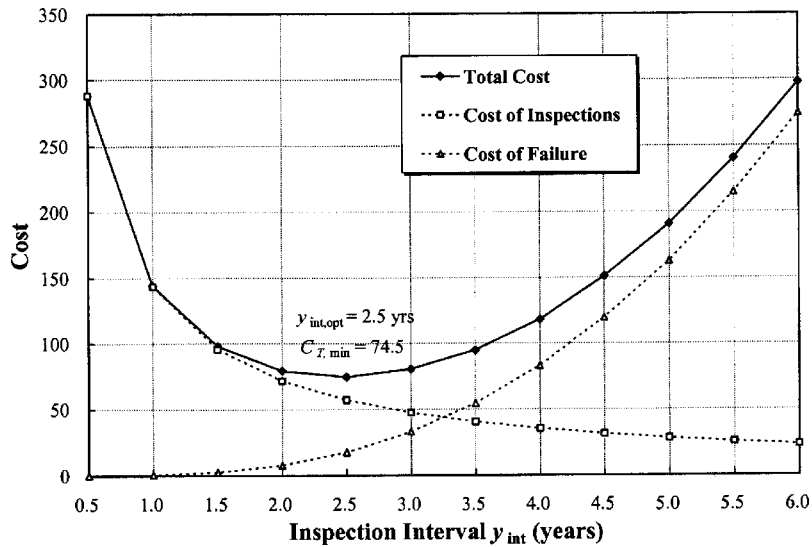


Fig. 17. Costs of ultrasonic inspections for various fixed-interval schedules for $K_{I,UI}:K_F=1.5:4 \times 10^4$

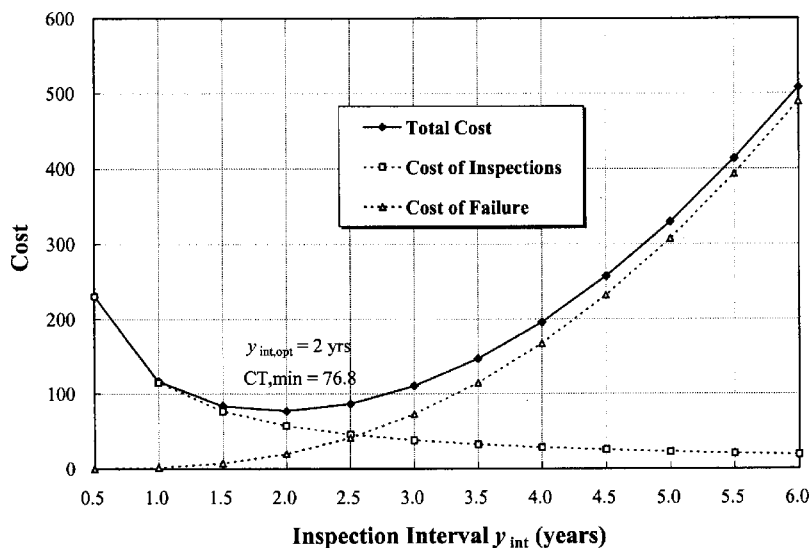


Fig. 18. Costs of magnetic particle inspections for various fixed-interval schedules for $K_{I,MI}:K_F=1.2:4 \times 10^4$

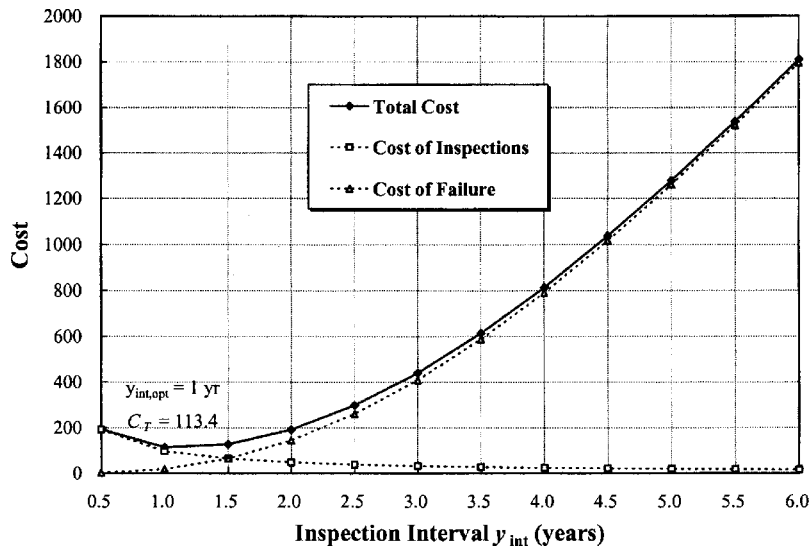


Fig. 19. Costs of penetrant inspections for various fixed-interval schedules for $K_{I,MI}:K_F=1.2:4 \times 10^4$

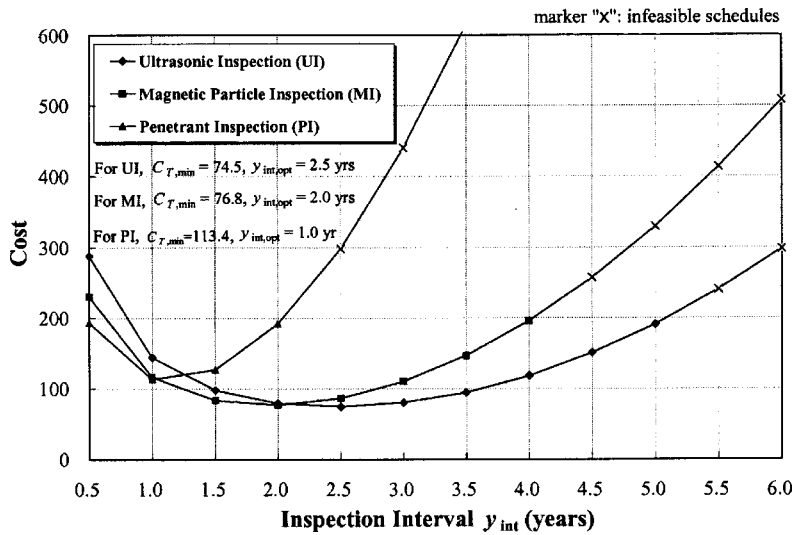


Fig. 20. Cost comparison of UI, MI, and PI in various fixed-interval schedules for $K_{I,PI}:K_{I,MI}:K_{I,UI}:K_F=1.0:1.2:1.5:4 \times 10^4$ (showing infeasible schedules when $P_{nd \max}=0.005$)

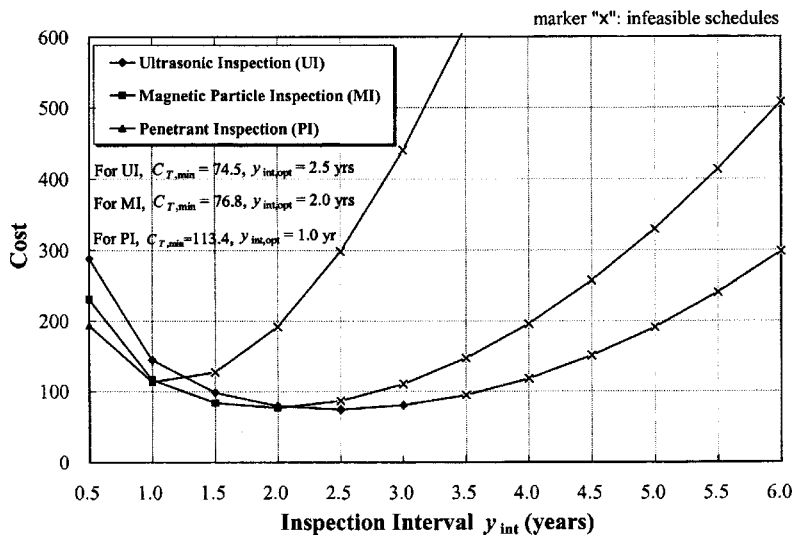


Fig. 21. Cost comparison of UI, MI, and PI in various fixed-interval schedules for $K_{I,PI}:K_{I,MI}:K_{I,UI}:K_F=1.0:1.2:1.5:4 \times 10^4$ (showing infeasible schedules when $P_{nd \max}=0.001$)

2. Comparing NDI techniques (as was done in Table 4), an NDI technique with a lower crack detectability will demand more inspections ($E[n]$) than one with a higher crack detectability to achieve the schedule with minimum total cost. This result is consistent with the practical experience where more inspections are needed for an NDI technique with a low crack detectability to ensure careful monitoring.
3. From the results of the numerical examples presented, it is seen that ideally the optimal inspection schedule for a fracture-critical member should consider the cost and quality of the NDI technique employed. If POD data for the fracture-critical member of interest are available for candidate NDI techniques, the procedure presented here can rationally (by including consideration for cost and safety) yield an optimal inspection schedule instead of any ad hoc periodic inspection schedule.
4. Optimization results are very directly affected by the NDI detectabilities (i.e., POD functions): the constraint on the largest permitted expected probability of not detecting a crack, $E[P_{nd}]$; and the relative costs of inspection and failure.
5. Regarding the effect of crack detectability, it can be seen, from the examples presented (such as in Fig. 14), that an NDI technique with higher detectability for cracks will tend to yield lower $E[P_{nd}]$ values. This in turn leads to lower costs of failure in the total cost. However, an NDI technique with a higher crack detectability is usually more expensive and will involve higher inspection costs.
6. Regarding the effect of the $P_{nd,max}$ constraint, it is found that by lowering the $P_{nd,max}$ value (i.e., raising the required safety level for a detail), schedules with longer time between inspections tend to become unacceptable because such schedules can cause higher $E[P_{nd}]$ values than the prescribed value of $P_{nd,max}$. Upon decreasing the $P_{nd,max}$ value, the optimal schedule adjusts to a shorter inspection interval. This observed trend is in agreement with experience where higher safety levels required for a detail must generally demand more frequent inspections (i.e., a shorter inspection interval).
7. Regarding the effect of the relative cost of failure, K_F , as can be seen in the two cases studied, higher relative costs of failure have a tendency to require schedules with shorter times between inspections. Comparing Figs. 11 and 17, for example, it can be seen that the higher K_F case lifts the failure cost curve and hence the total cost curve when costs are studied versus inspection interval. The K_F value does not, however, affect the expected number of inspections $E[n]$ in any schedule; hence, the inspection cost curve remains unchanged. The raised total cost curve due to the increased failure cost curve shifts the optimal schedule to one with a shorter inspection interval. In addition, with higher K_F values, higher crack detectability becomes more important

in the optimal NDI technique. This is because an NDI technique with a higher crack detectability will usually lead to lower failure costs.

Acknowledgment

The writers gratefully acknowledge financial support through a research grant awarded by the Texas Department of Transportation as part of Project No. 0-2135, Inspection Guidelines for Fracture-Critical Steel Trapezoidal Girders.

References

- Berens, A. P. (1989). "NDE reliability analysis." *Metals handbook*, 9th Ed., Vol. 17, ASM International, Materials Park, Ohio, 689–701.
- Berens, A. P., and Hovey, P. W. (1981). "Evaluation of NDE reliability characterization." *AFWAL-TR-81-4160*, Vol. 1, Air Force Wright-Aeronautical Laboratory, Wright-Patterson Air Force Base, Dayton, Ohio.
- Cramer, E. H., and Friis-Hansen, P. (1992). "Reliability based optimization of multi-component welded structures." *Proc., 11th Int. Conf. on Offshore Mechanics and Arctic Engineering*, Vol. 2, ASME, New York, 265–271.
- Faber, M. H., Sorensen, J. D., and Kroon, I. (1992). "Optimal inspection strategies for offshore structural systems." *Proc., 11th Int. Conf. on Offshore Mechanics and Arctic Engineering*, Vol. 2, ASME, New York, 145–151.
- Hartle, R. A., Amrhein, W. J., Wilson, K. E., III, Bauhman, D. R., and Tkacs, J. J. (1995). "Bridge inspector's training manual 90." *FHWA-PD-91-015*, Federal Highway Administration, Washington, D.C.
- Johnson, R. A. (2000). *Miller and Freund's probability and statistics for engineers*, 6th Ed., Prentice-Hall, Upper Saddle River, N.J.
- Madsen, H. O., Krenk, S., and Lind, N. C. (1985). *Methods of structural safety*, Prentice-Hall, Englewood Cliffs, N.J.
- Miner, M. A. (1945). "Cumulative damage in fatigue." *J. Appl. Mech.*, 12(3), 159–164.
- Paris, P. C., and Erdogan, F. (1963). "A critical analysis of crack propagation laws." *J. Basic Eng.*, 85, 528–534.
- Rummel, W. D. (1998). "Probability of detection as a quantitative measure of nondestructive testing end-to-end process capabilities." *Mater. Eval.*, 56(1), 29–35.
- Rummel, W. D., and Matzkanin, G. A. (1997). *Nondestructive evaluation capabilities data book*, Nondestructive Testing Information Analysis Center, Austin, Tex.
- Schilling, C. G., Klippstein, K. H., Barsom, J. M., and Blake, G. T. (1978). "Fatigue of welded steel bridge members under variable-amplitude loadings." *National Cooperative Highway Research Program Rep. No. 188*, Transportation Research Board, National Research Council, Washington, D.C.
- Sorensen, J. D., Faber, M. H., Rackwitz, R., and Thoft-Christensen, P. (1991). "Modeling in optimal inspection and repair." *Proc., 10th Int. Conf. on Offshore Mechanics and Arctic Engineering*, Vol. 2, ASME, New York, 281–288.